Pyrovanadolysis, a Pyrophosphorolysis-like Reaction Mediated by Pyrovanadate, Mn2+, and DNA Polymerase of Bacteriophage T7

Akabayov, Barak; Kulczyk, Arkadiusz W.; Akabayov, Sabine R.; Theile, Christopher; McLaughlin, Larry W.; Beauchamp, Benjamin; van Oijen, Antoine M.; Richardson, Charles C.

Published in:
The Journal of Biological Chemistry

DOI:
10.1074/jbc.M111.250944

Publication date:
2011

SUPLLEMENTAL DATA

PYROVANADOLYSIS: A PYROPHOSPHOROLYSIS-LIKE REACTION MEDIATED BY PYROVANADATE, MN^{2+}, AND DNA POLYMERASE OF BACTERIOPHAGE T7

Barak Akabayov[1], Arkadiusz W. Kulczyk[1], Sabine R. Akabayov[1], Christopher Theile[2], Larry W. McLaughlin[2], Benjamin Beauchamp[1], and Charles C. Richardson[1]

From the Department of Biological Chemistry and Molecular Pharmacology[1], Harvard Medical School, 240 Longwood Ave., Boston, MA, and the Department of Chemistry[2], Merkert Chemistry Center, Boston College, Chestnut Hill, Massachusetts 02467, USA

Running head: Pyrovanadolysis by the T7 DNA polymerase

Address correspondence to: Charles C. Richardson, Department of Biological Chemistry and Molecular Pharmacology, Harvard Medical School, 240 Longwood Ave., Boston, MA 02115. Tel.: 617-432-1864; Fax: 617-432-3362; E-mail: ccr@hms.harvard.edu

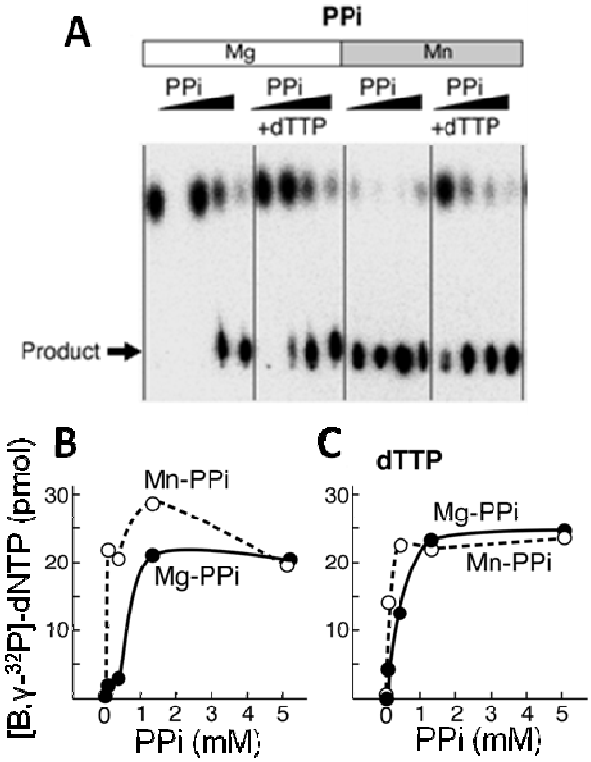

Supplemental Figure S1:

Pyrophosphorolysis and PPi exchange by Mn-substituted T7 DNA polymerase. *A*. Each pyrophosphorolysis reaction was performed as in Figure 3 using the recessed primer annealed to the DNA template with the following modifications: same amount of [32P]-PPi and varying amounts (0, 0.25, 1, 4 mM) of PPi in the absence or presence of 5 mM dTTP, to induce pyrophosphorolysis or PPi-exchange in the presence of 10 mM MgCl2 or 1mM MnCl2. After incubation for 10 minutes at 37 °C 0.4 μL of the reaction mixture was spotted onto PEI cellulose TLC plate and developed using 0.5 M LiCl, 0.5 M Na-formate. To better separate the [32P] PPi used in the reaction from the accumulated product ([32P] dNTP) we have coupled the reaction to pyrophosphatase (0.1 units). The radioactive products (dTTP) were visualized using autoradiography. *B*. Graphs represent quantification of dNPPP formation from the

pyrophosphorolysis reaction when increasing amounts of unlabeled PPi are present. (c) Graphs represent quantification of dNPPP formation from the PPi-exchange reaction when increasing amounts of unlabeled PPi are present.

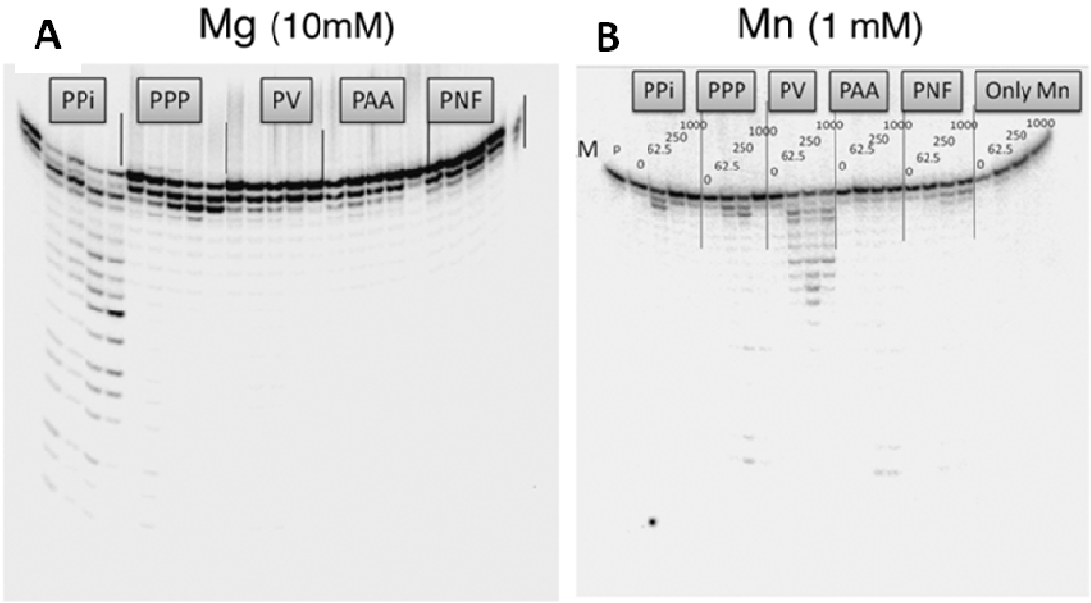

Supplemental Figure S2:

Ability of compounds that mimic PPi to mediate a pyrophosphorolysis-like reaction. Each of the compounds: triphosphate, VV, phosphonoformate, and phosphonoacetate, were added to the reaction mixture in varying amounts (0, 0.065, 0.25, and 1 mM) in the presence of 10 mM $MgCl_2$ (*A*) or 1 mM $MnCl_2$ (*B*). The reaction mixture contained 100 nM T7 gp5-D5D65/trx, deficient in 3' to 5' exonuclease activity, and 5 nM [5'-^{32}P] DNA primer (21-mer, 5'-CGAAAACGACGGCCAGTGCCA-3') annealed to template (26-mer, 5'-CCCCTTGGCACTGGCCGTCGTTTTCG-3'), 40 mM Tris-HCl (pH 7.5) 10 mM, 10 mM DTT, and 50 mM potassium glutamate. After incubation at 37 °C for 20 minutes the radioactive products were analyzed by electrophoresis through a 25% polyacrylamide gel containing 3 M urea and visualized using autoradiography.

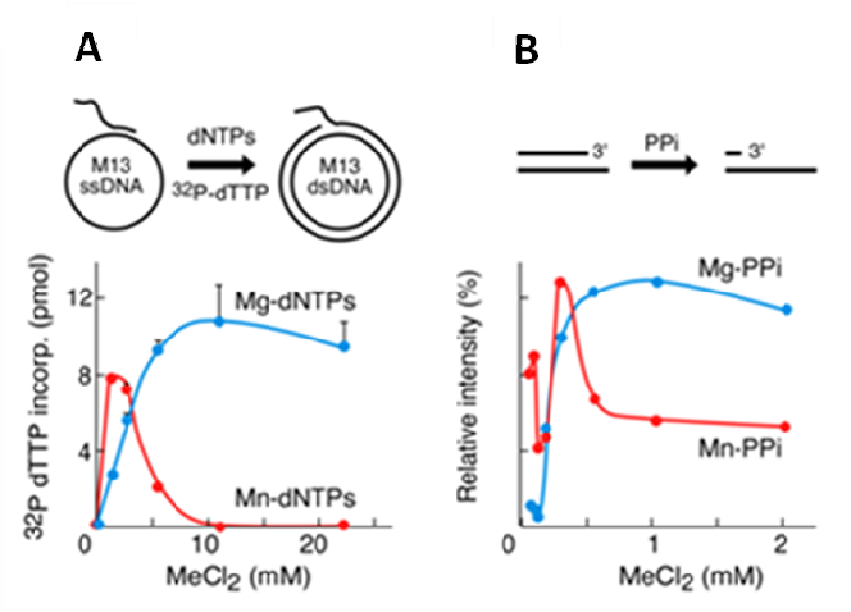

Supplemental Figure S3:

Effect of Mg or Mn on polymerization and pyrophosphorolysis activities. *A*. Polymerase activity was measured in the standard DNA polymerase assay containing 40 mM Tris-HCl, pH 7.5, 10 mM DTT, 50 mM potassium glutamate, 0.25 mM dTTP, dCTP, dGTP, and [α-^{32}P] dATP, 20 nM primed M13 DNA, and 5 nM gp5/trx, at the indicated concentrations of $MgCl_2$ (blue) or $MnCl_2$ (red). After incubation at 37 °C for 10 min the amount of [α-^{32}P] dAMP incorporated into DNA was measured. *B*. Pyrophosphorolysis was performed as in Supporting Figure 1 and the bands in the gels presented in (c, marked in arrow) were analyzed using Adobe Photoshop and the method described in http://lukemiller.org/journal/2007/08/quantifying-western-blots-without.html.

Results in the presence of Mg^{2+} and Mn^{2+} in the reaction mixture are indicated in blue and red, respectively.

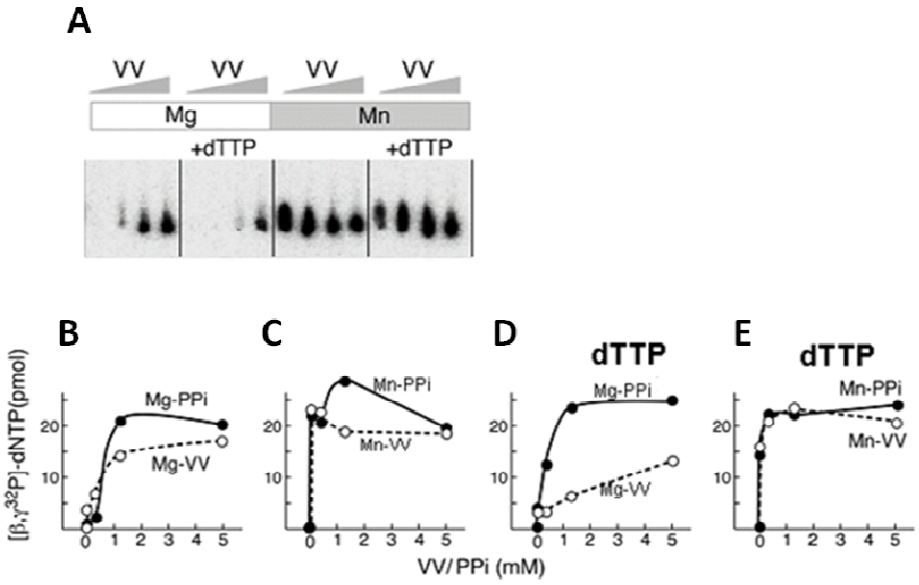

Supplemental Figure S4:

Competition effect between VV and [^{32}P]-PPi by T7 DNA polymerase. *A*. The pyrophosphorolysis reaction was performed as in Supplemental Figure 1 using the recessed primer annealed to the DNA template with the following modifications: varying amounts (0, 0.25, 1, 4 mM) of VV to constant concentration of [^{32}P]-PPi. After incubation for 10 minutes at 37 °C 0.4 μL of the reaction mixture was spotted onto PEI cellulose TLC plate and developed using 0.5 M LiCl, 0.5 M Na-formate. To better separate the [^{32}P]-PPi used in the reaction from the accumulated product ([^{32}P]-dNTP) we have coupled the reaction to pyrophosphatase (0.1 units). The radioactive products (dTTP) were visualized using autoradiography. Graphs represent quantification of dNPPP formation at the end of the pyrophosphorolysis reaction when increasing amounts of unlabeled VV are present (*B*-*E*). VV competes with labeled PPi on binding to Mg as indicated from pyrophosphorolysis (*B*) or PPi exchange (*D*). VV fail to compete effectively with labeled PPi when Mn is present, in the absence (*C*) or presence of the next incoming nucleotide (*E*).

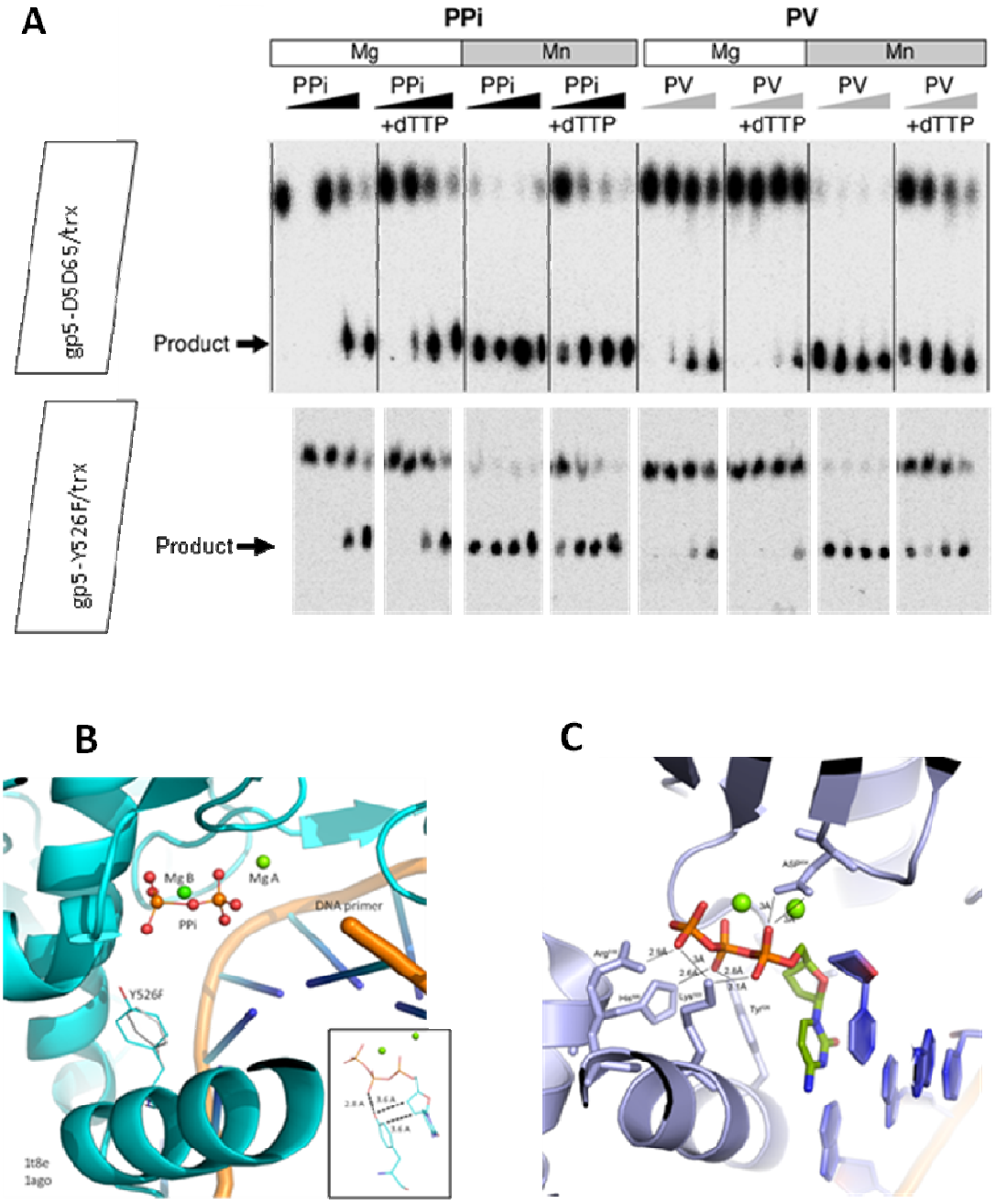

Supplemental Figure S5:

Pyrophosphorolysis product formation by gp5/trx (gp5-Y526F/trx) using Mg^{2+} and Mn^{2+} and the competition effect by VV. *A.* The pyrophosphorolysis reaction was performed as in Supplemental Figure 1 using the recessed primer annealed to the DNA template with the

following modifications: varying amounts (0, 0.25, 1, 4 mM) of VV to constant concentration of [^{32}P]-PPi. After incubation for 10 minutes at 37 °C 0.4 μL of the reaction mixture was spotted onto PEI cellulose TLC plate and developed using 0.5 M LiCl, 0.5 M Na-formate. To better separate the [^{32}P]-PPi used in the reaction from the accumulated product ([^{32}P]-dNTP) we have coupled the reaction to pyrophosphatase (0.1 units). The radioactive products (dTTP) were visualized using autoradiography. Top panel represents the reaction using T7 DNA polymerase (gp5-D5D65/trx), bottom represents the reaction using gp5-Y526F/trx. *B.* Model of the active site of gp5 (PDB entry 1T8E). The active site is shown with two Mg^{2+} ions (green), PPi from an overlay of the two metal ions in Dpo4 crystal structure together with PPi (PDB entry 2ago), and the Y526 at the O-helix. The structural alignment and figure preparation were created using PyMOL (http://www.pymol.org). Inset shows the proximity of Y526 to the hydroxyl phosphate (Pβ) of the incoming nucleotide. *C.* Residues in closed proximity to the nucleotide (PDB entry 1T8E). The active site is shown with two Mg2+ ions (green), nucleotide the following amino acids at the O-helix that are in closed proximity to the phosphate backbone of the incoming nucleotide: Arg518, His506, Lys522, Tyr526, Asp654. The structural alignment and figure preparation were created as in *B*.

Supplemental Table S1:

Distance of terminal and bridging oxygens in phosphorus or vanadium, distance of P-P or V-V, and the angle of the bridging oxygen (POP, VOV). The measurements obtained from available crystal structures of representative molecules free or bound to an enzyme active site.

	A	B	C	D
PPi(1)	1.52	1.59	3	144
VV(2)	1.69	1.8	3.4	141
$P_\beta P_\gamma$ of ddGTP, T7 DNA polymerase(3)	1.5	1.6	3	151
PPi, Y family DNA polymerase Dpo4(4)	1.5	1.9	3.2	140
VV, Yersinia protein-tyrosine phosphatase YopH(5)	1.9	2.1	3.1	102

A: Terminal (O), P-O or V-O average bond length (Å)

B: Bridging (O), P-O or V-O average bond length (Å)

C: P-P or V-V distance (Å)

D: Angle POP or VOV (°)

REFERENCES

1. Calvo, C. (1967) *Acta Cryst* 23, 289-295
2. Holloway, C. E., and Melnick, M. (1985) *Rev Inorg Chem* 8, 287-360
3. Doublie, S., Tabor, S., Long, A. M., Richardson, C. C., and Ellenberger, T. (1998) *Nature* 391, 251-258
4. Vaisman, A., Ling, H., Woodgate, R., and Yang, W. (2005) *EMBO J* 24, 2957-2967
5. Brandao, T. A., Robinson, H., Johnson, S. J., and Hengge, A. C. (2009) *J Am Chem Soc* 131, 778-786